International High Performance Buildings Conference

School of Mechanical Engineering

July 2018

# Preliminary Assessment of a Weather Forecast Tool for Building Operation

José Agustín Candanedo
*CanmetENERGY-Varennes, Canada*, jose.candanedoibarra@canada.ca

Jean-Marc Hardy
*CanmetENERGY-Varennes, Canada*, jean-marc.hardy@canada.ca

Étienne Saloux
*CanmetENERGY-Varennes, Canada*, etienne.saloux@canada.ca

Radu Platon
*CanmetENERGY-Varennes, Canada*, radu.platon@canada.ca

Vahid Raissi-Dehkordi
*CanmetENERGY-Varennes, Canada*, vahid.raissidehkordi@canada.ca

***See next page for additional authors***

**Authors**
José Agustín Candanedo, Jean-Marc Hardy, Étienne Saloux, Radu Platon, Vahid Raissi-Dehkordi, and Alexandre Côté

# Preliminary Assessment of a Weather Forecast Tool for Building Operation

José A. CANDANEDO[1]*, Étienne SALOUX[1], Jean-Marc HARDY[1], Radu PLATON[1],
Vahid RAISSI-DEHKORDI[1], Alexandre CÔTÉ[1]

[1]CanmetENERGY, Natural Resources Canada
Varennes, QC, CANADA
Phone : (450) 652-3126; Fax : (450) 652-5177; E-mail : jose.candanedoibarra@canada.ca

* Corresponding Author

## ABSTRACT

Model-based predictive control (MPC) offers significant opportunities for building operation. However, it must overcome several obstacles to facilitate its widespread adoption. One of these obstacles is the lack of user-friendly weather forecast tools tailored for the implementation of MPC in building operation. This paper discusses the development of a weather forecast tool targeting this issue and a preliminary assessment of its accuracy. This tool uses raw forecast data from the Canadian national meteorological service as an input to create tables of data with a prediction horizon of 48 hours. High spatial resolution data makes it possible to obtain forecasts for a very specific geographic location. A post-processing treatment is used to obtain estimates of solar radiation on different planes of interest, such as façades, roofs or building-integrated photovoltaic installations. The forecast data can be obtained automatically at 6-hour intervals. An overview of the tool and its features is presented. An estimation of the accuracy of the weather forecasts is carried out by comparing predicted weather data with actual measurements in Canadian sites. Finally, possible future upgrades for the tool are discussed.

## 1. INTRODUCTION

In recent years, model-based predictive control (MPC) has received significant attention from the research community due to its potential to improve the operation of buildings (Aswani et al., 2012; Corbin et al., 2013; Drgoňa et al., 2018; Hu and Karava, 2014; Killian and Kozek, 2016; Oldewurtel et al., 2012). MPC uses models of the building and its system, along with forecasts of weather and occupant behaviour, to run optimization algorithms targeting the selection of optimal control actions for a given objective. MPC applications include, among others: temperature setpoint adjustment in anticipation of weather changes; regulation of the charge or discharge of energy storage devices; control of the temperature of thermally-active building systems (TABS), control of motorized blinds according to expected solar gains; and regulation of the building-grid interaction.

Despite numerous studies confirming its potential, MPC is still far from being a mainstream practice in building operation. One of the reasons why MPC has fallen short of expectations is the lack of tools for incorporating weather forecast data in building automation systems in a straightforward manner. With a few exceptions, such as the efforts carried out by MeteoSwiss (Stauch et al., 2010) there is a scarcity of tools designed for this purpose.

In view of this, efforts have been conducted in our centre in this direction. An early attempt focused on the periodic creation of EnergyPlus weather files (EPW) (Candanedo et al., 2013). However, over the last few years a more general tool –suitable for any simulation environment or building automation system- has been targeted. The objective was to facilitate the periodic generation of tables containing weather forecast data that would be easy to access, would contain numerous variables, and would be available for any point in the Canadian territory. Furthermore, it was important to include the capability to obtain solar irradiance forecasts on planes with different azimuths and slopes, so that the tool could be used to estimate solar heat gains in buildings and the generation of building-integrated photovoltaic systems. Finally, it was important to make this tool as user-friendly and practical as possible. CanMETEO was publicly released, free of charge, in August 2017 (*CanMETEO*, 2017).

This paper describes the methodology used by CanMETEO to retrieve weather forecast information, as well as the main features of the software tool. It also presents a preliminary assessment of its performance by comparing its predictions with measured data at two Canadian locations. Plans for future improvements to the tool are discussed.

## 2. METHODOLOGY

Meteorological services around the world make use of numerical weather prediction (NWP) models. NWPs are simulations of the atmosphere carried out by discretizing a large 3D domain into hundreds of thousands of control volumes (Bauer et al., 2015). Continuity, momentum and energy balance equations are solved for each of these domains at discrete time steps. The boundary conditions are obtained from satellite imagery and measurements from terrestrial stations. The solution of these systems of millions of equations is among the most computationally demanding tasks carried out nowadays. National weather services perform these simulations by using Gridded Binary (GRIB) files, a compact binary format that facilitates the handling of large meteorological datasets. The Canadian Meteorological Centre runs NWP models periodically. The raw results (in GRIB format) are made freely available to the public. The GRIB file results are then used by commercial weather forecast companies to perform some post-processing to add additional information and make the results accessible to the public. These weather services tend to focus on populated areas, and target specific variables, such as temperature, humidity, precipitation or wind speed. While these forecasts usually indicate cloud cover conditions (e.g., sunny, overcast, etc.), quantitative solar irradiance variables are not available. Thus, the tool focuses on three goals:

- Providing a graphical interface to facilitate the selection of a specific geographical location and variables of interest, including solar irradiance on different planes;
- Converting the GRIB files into an accessible format (CSV files) and;
- Providing solar irradiance estimates at hourly intervals that may be used for calculations of solar gains and the output of PV arrays.

### 2.1 Geographical Location and Selection of Variables of Interest

CanMETEO uses numerical weather prediction GRIB files that are posted every 6 hours by Environment Canada. High resolution GRIB files provide high spatial density (i.e. grids of 2.5 km x 2.5 km at the ground level, and even denser in urban areas), covering most of the Canadian territory and regions in the United States (Figure 1).

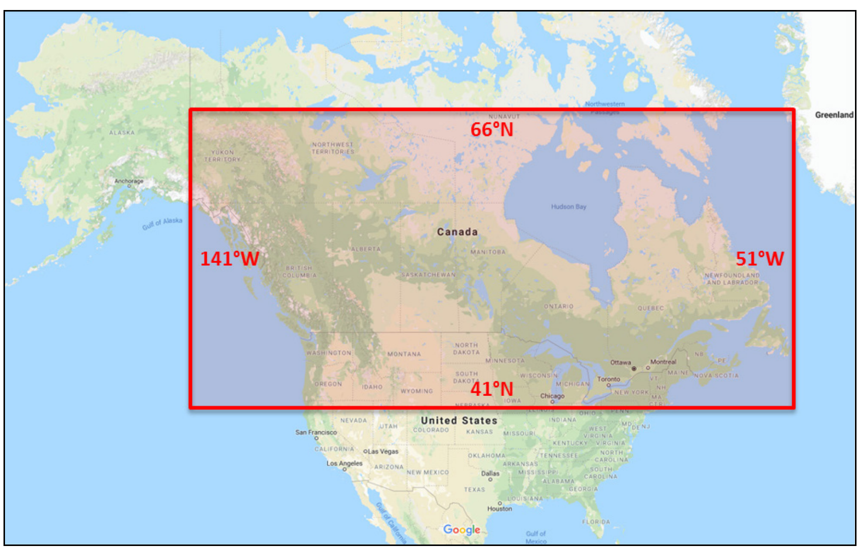


**Figure 1.** Data Availability of CanMETEO.

The graphical interface of the tool enables zooming in and out to select a particular location (latitude and longitude). The geographic coordinates can also be entered manually (Figure 2). The user can also select the forecast variables to be included in the output CSV file. By default, temperature, specific humidity, wind speed and cloud cover will be reported. The user can also specify solar irradiance on different planes after providing the azimuth (0° for due South) and inclination of the plane (between 0° and 90°). Other available variables include: albedo, dew point, precipitation, global horizontal and diffuse horizontal radiation.

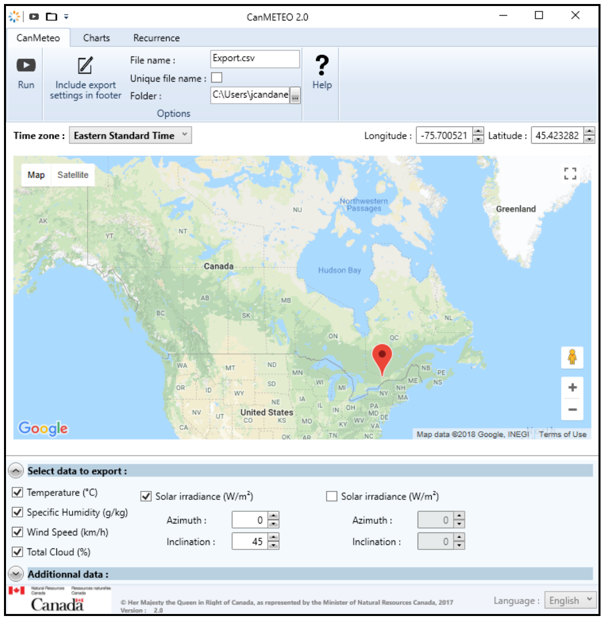


**Figure 2.** CanMETEO opening screen.

## 2.2 Estimation of Solar Irradiance on Different Planes

The calculation of the direct irradiance on any given plane of interest (e.g., a roof or a façade) requires some basic astronomical calculations to determine the position of the Sun relative to the plane. A detailed explanation of these calculations can be found in Duffie and Beckman (Duffie and Beckman, 2006).

In order to estimate the diffuse irradiance on any given plane, the diffuse horizontal ($G_{dh}$) and direct beam ($I_b$) radiation are required as inputs. However, these two values are not released by default in the output of a NWP file; typically, the "cloudiness" of the sky is given as "cloud cover", a value between 0 and 100%. To circumvent this issue is thus necessary, an empirical correlation proposed by Samimi (2015) is applied to calculate the location turbidity ($T_L$).

$$T_L = 0.8 \cdot \left(0.01 * CloudCover\right) + 0.2 \tag{1}$$

This value is used to calculate the atmosphere transmittance ($\tau_{atm}$) and the beam radiation ($I_b$). With this information, the direct beam and the diffuse horizontal values can be obtained. The Perez model (Perez et al., 1990) is then applied to calculate the diffuse solar radiation on a given surface. With this information, the total radiation on a surface is the sum of the diffuse radiation, the beam radiation component (beam radiation times the cosine of the angle of incidence) and the reflected radiation from the ground. The albedo ($\rho$) from the NWP file is used.

$$G_{\mathrm{surface}} = G_{\mathrm{dif\_Perez}} + I_b \cos(\theta) + 0.5 \rho G_{gh} \tag{2}$$

where $G_{surface}$ is the total solar radiance received by the surface, $G_{dif\_Perez}$, is the diffuse radiation on that surface as calculated by the Perez model, $G_{gh}$ is the global horizontal radiation for the site, and $\theta$ is the incidence angle of the direct radiation on the surface.

## 2.3 Output files and Charts

The output of CanMETEO is created in a CSV file with 48 rows, corresponding to the 48-hour horizon of the GRIB file. The user has the possibility of indicating whether to include additional information in the header (such as location, the time when the forecast was released). Figure 3 shows a fragment of a typical CSV output file. The "time stamps" for the hourly data include both the UTC time (used by convention in NWP) and the local time.

| | A | B | C | D | E | F | G |
|---|---|---|---|---|---|---|---|
| 1 | UTC time | Local time | Custom Orientation Azimuth: 0 Inclinaision : 45[W/m²] | Specific Humidity[g/kg] | Temperature[°C] | Total Cloud[%] | Wind Speed[km/h] |
| 2 | 05/03/2018 06:00 | 05/03/2018 01:00 | 0 | 3.105770826 | -1.112670898 | 57.53326035 | 16.51648331 |
| 3 | 05/03/2018 07:00 | 05/03/2018 02:00 | 0 | 3.18138051 | -1.468353271 | 56 | 10.62689209 |
| 4 | 05/03/2018 08:00 | 05/03/2018 03:00 | 0 | 3.1708951 | -1.406494141 | 57.80199051 | 9.781683922 |
| 5 | 05/03/2018 09:00 | 05/03/2018 04:00 | 0 | 3.154040337 | -1.305969238 | 71.33525085 | 9.61285305 |
| 6 | 05/03/2018 10:00 | 05/03/2018 05:00 | 0 | 3.127840757 | -1.324066162 | 80 | 9.219488144 |
| 7 | 05/03/2018 11:00 | 05/03/2018 06:00 | 0 | 3.091714144 | -1.416656494 | 80 | 9.545777321 |
| 8 | 05/03/2018 12:00 | 05/03/2018 07:00 | 23.474608 | 3.080234051 | -1.244934082 | 88 | 9.897356987 |
| 9 | 05/03/2018 13:00 | 05/03/2018 08:00 | 91.62647758 | 3.239190102 | -0.114837646 | 80 | 10.69602299 |
| 10 | 05/03/2018 14:00 | 05/03/2018 09:00 | 340.6897531 | 3.326107502 | 1.053436279 | 40.48968887 | 12.6256609 |
| 11 | 05/03/2018 15:00 | 05/03/2018 10:00 | 669.2312267 | 3.276259422 | 1.64755249 | 28.48968887 | 14.1574173 |
| 12 | 05/03/2018 16:00 | 05/03/2018 11:00 | 910.0931849 | 3.307067394 | 2.284484863 | 16.0783844 | 15.3862009 |
| 13 | 05/03/2018 17:00 | 05/03/2018 12:00 | 607.8741271 | 3.363512754 | 2.646392822 | 56.08216476 | 15.62123108 |
| 14 | 05/03/2018 18:00 | 05/03/2018 13:00 | 374.7343012 | 3.352845907 | 2.563079834 | 92 | 14.50226879 |
| 15 | 05/03/2018 19:00 | 05/03/2018 14:00 | 311.2882183 | 3.282915115 | 2.235412598 | 92 | 14.25447845 |
| 16 | 05/03/2018 20:00 | 05/03/2018 15:00 | 547.0338441 | 3.296547174 | 2.432617188 | 28.8927803 | 13.40927982 |
| 17 | 05/03/2018 21:00 | 05/03/2018 16:00 | 414.0967873 | 3.348564148 | 2.534912109 | 0 | 13.10352612 |
| 18 | 05/03/2018 22:00 | 05/03/2018 17:00 | 112.9112094 | 3.272967815 | 1.427947998 | 0 | 11.04344845 |
| 19 | 05/03/2018 23:00 | 05/03/2018 18:00 | 0 | 3.120066166 | -0.215911865 | 0 | 10.09578991 |
| 20 | 06/03/2018 00:00 | 05/03/2018 19:00 | 0 | 2.98395443 | -1.170257568 | 0 | 9.676879883 |
| 21 | 06/03/2018 01:00 | 05/03/2018 20:00 | 0 | 2.975591898 | -1.294769287 | 58.04737854 | 10.30741787 |
| 22 | 06/03/2018 02:00 | 05/03/2018 21:00 | 0 | 3.047396421 | -0.935272217 | 86.99712372 | 10.11414623 |

**Figure 3.** Typical CSV output file.

Apart from the CSV tables, the software shows charts that facilitate the interpretation by the building operator (Figure 4). The graphs contain a vertical line that displays the current moment (i.e., the moment when the graphs are being accessed). There is often a short delay between the initial time ($t_o$) in the output and the moment when the forecast is displayed. While the graphical information shown in the charts may be useful for the interpretation of data, the CSV tables remain the key output, since they can be easily accessed by a control algorithm.

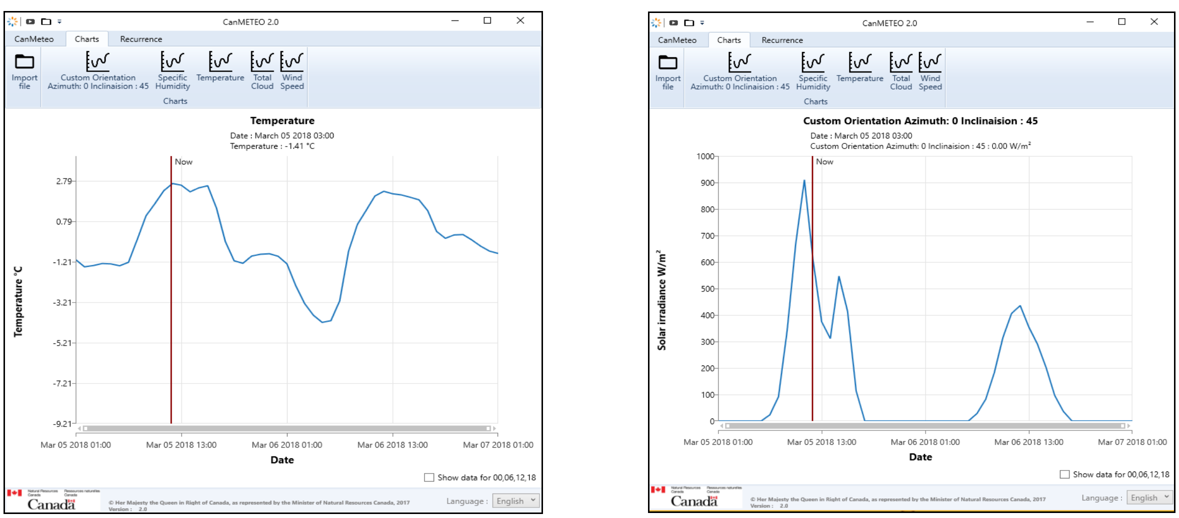


**Figure 4.** Typical charts in CanMETEO: temperature and solar irradiance on a south-facing surface with a 45° inclination angle. The red line indicates the time when the charts were plotted.

## 3. WEATHER FORECAST ACCURACY

In this section, the accuracy of weather forecasts is assessed for two different locations: Varennes (Québec) and Okotoks (Alberta). Weather forecasts and measured data are first presented and discussed. Then, the accuracy of predicted ambient temperature and solar radiation is evaluated for a period of six months (Jul-Dec 2017). Since the solar radiation forecast appears overestimated, a post-processing procedure is finally presented.

### 3.1 Measured data and weather forecast database

To assess the accuracy of weather forecasts, real measurements are necessary. Thus, forecasts were compared with measured data for two locations: the site of the research centre where CanMETEO was developed in the municipality of Varennes (near Montréal, Québec), and Okotoks (near Calgary, Alberta) the city that hosts the Drake Landing Solar Community (DLSC) (Sibbitt et al., 2012). The sites were chosen due to the availability of high resolution and reliable monitoring weather data.

For these locations, ambient temperature and solar radiation measurements (on horizontal and 45°-tilted, with a due South azimuth) are available at 1-min intervals for Varennes and 10-min intervals for Okotoks. At Varennes, the measurements were obtained with recently calibrated instruments. In the case of the Drake Landing community, it is assumed that the pyranometers are well calibrated since the weather conditions are continuously monitored and used for operational purposes. The period analyzed in this study is July 1$^{st}$ - December 31$^{st}$, 2017.

### 3.2 Considerations in the evaluation of accuracy

Evaluating forecast accuracy presents some challenges that are not evident at first glance. To start, as previously mentioned, forecasts are available on an hourly basis for 48-hr horizon, and released by Environment Canada every 6 hours. Therefore, several predictions exist for the same moment in time, obtained from different forecasts (up to 9 values). For comparison purposes, hourly averaged values have been calculated for the data when necessary by considering that the predicted value given at time $t_o$ refers to the next hour, i.e., [$t_o$, $t_o$+1]. Moreover, forecast accuracy can be evaluated according to several mathematical criteria.

The accuracy of ambient temperature forecasts can be satisfactorily evaluated by comparing instantaneous hourly values. In contrast, using instantaneous solar radiation values can yield significant differences (which may be due, for example, to the short-term effects of clouds). Thus, this criterion is not as important as the total energy received over a certain period (e.g., the next 6, 24 or 48 hours). These criteria are discussed in the next sections.

Note that the graphs shown here represent typical results, not those that provide the best fit. Moreover, only 45°-tilted solar radiation is analyzed but similar results have been obtained for the irradiance on a horizontal plane.

### 3.3 Accuracy of ambient temperature forecasts

In CanMETEO weather forecasts, predictions are given for the next hour and up to 48-hr ahead. It is reasonable to expect predictions for shorter prediction horizons to be more accurate. Figure 5 compares measured and predicted ambient temperatures at Okotoks for different prediction horizons. "Forecast 1-hr", meant as a reference, corresponds to the hour immediately following the initial time of the forecast ($t_o$); the "Forecast 6-hr" corresponds to the six (6) values following the release of the forecast; finally, "Forecast 48-hr" corresponds to the 48 values following the release of the forecast. From this figure, it can be seen that the ambient temperature is predicted within reasonable accuracy over the 48-hr horizon, even though larger deviations are occasionally observed (e.g., Sep-28).

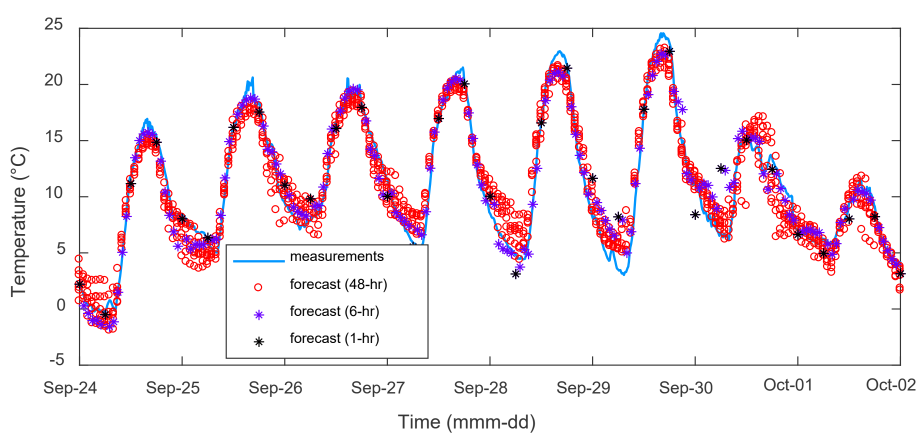


**Figure 5.** Forecast ambient temperature in Okotoks.

These results are confirmed in a scatter plot of predicted vs measured temperatures (Figure 6) for Okotoks. Most of the 6-hr ahead predictions are within the range of +/-3°C; deviations can be larger for the 48-hr ahead forecast. A histogram of the difference between the predicted and measured ambient temperature is also given and illustrates the accurate predictions (Figure 7). The mean value of the error is close to 0°C and the standard deviation is 2.2°C.

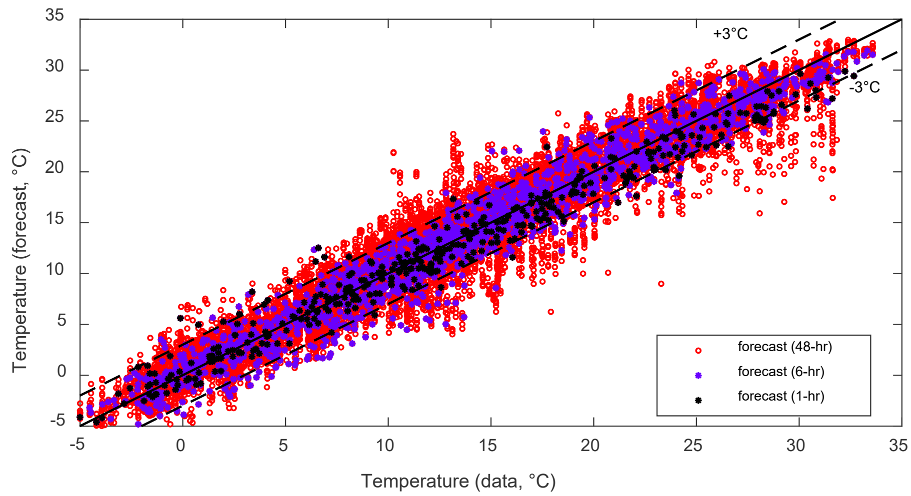


**Figure 6.** Comparison between forecasts and data for ambient temperature in Okotoks.

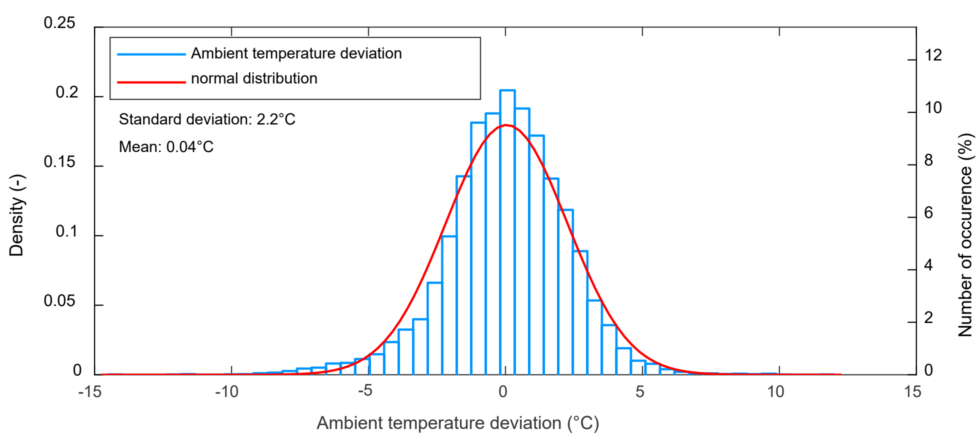


**Figure 7.** Histogram of ambient temperature errors (predicted – measured).

The accuracy of ambient temperature forecasts was evaluated by using two indicators:

- the *root-mean-square deviation* (RMSD):

$$\text{RMSD [°C]} = \sqrt{\frac{1}{N_T \sum_{i=1}^{N_T} n_{T,i}} \sum_{i=1}^{N_T} \sum_{j=1}^{n_{T,i}} \left(T_{\text{amb},i,j}^{\text{fore}} - T_{amb,i}^{\text{meas}}\right)^2} \quad (3)$$

- the *forecast spread* $\Delta T_{\text{amb,max},i}^{\text{fore}}$ between the maximum and minimum values predicted for the same time $t_i$ :

$$\Delta T_{\text{amb,max},i}^{\text{fore}} [°\text{C}] = \max\left(T_{\text{amb},i,j}^{\text{fore}}\right) - \min\left(T_{\text{amb},i,j}^{\text{fore}}\right) \quad (4)$$

where:

- ○ $T_{\text{amb},i}^{\text{meas}}$ is the hourly measured ambient temperature at a given time $t_i$
- ○ $T_{\text{amb},i,j}^{\text{fore}}$ is the hourly predicted ambient temperature for the time $t_i$ for the $j$ forecast horizons (each time $t_i$ may have up to 9 values).

- $N_T$ is the total number of measured values over the entire period of interest
- $n_{T,i}$ is the total number of predictions available for each time $t_i$ (varying between 1 and 9)

Table 1 shows the results for Okotoks and Varennes. It is worth mentioning that similar results were obtained for both Okotoks and Varennes. The deviation of all forecasts was evaluated at about 2°C (2.2°C for Okotoks, 2.3°C for Varennes), which is consistent with the results shown in Figure 7. Moreover, the forecast spread obtained from the different forecasts for the same time is <3°C on average, although but it can reach up to more >10°C (12.6°C for Okotoks, 11.1°C for Varennes). On the other hand, such a large difference was reached only a few times during the studied period; deviations larger than 8°C were obtained for less than 3% of the measurements (3% for Okotoks, 0.5% for Varennes) and is mainly due to preliminary underestimation or overestimations. For instance, the ambient temperature measured in Okotoks was 31.6 °C on July 23rd at 17:00. The temperature predicted 16-hours ahead was 17.4 °C, quite far from the real value; however, the forecast four hours ahead was 30.0 °C, a much better estimation. In general, temperature forecasts are quite reliable and accurate.

**Table 1:** Accuracy of ambient temperature forecasts (July 1st – December 31st)

| Indicator | | Okotoks (AB) | Varennes (QC) |
|---|---|---|---|
| RMSD | | 2.2°C | 2.3°C |
| Forecast spread | Mean value | 2.8°C | 2.4°C |
| | Max value | 12.6°C | 11.1°C |

### 3.4 Accuracy of solar radiation forecasts

A similar approach was applied to solar radiation forecasts (*i.e.*, 1-hr, 6-hr and 48-hr ahead), which are shown in Figure 8 for Okotoks.

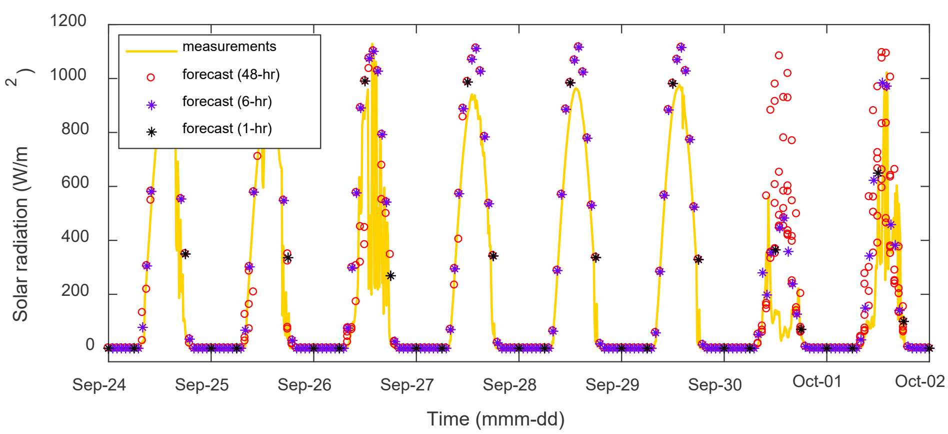


**Figure 8**. Raw forecasts, due South, 45°-tilted solar radiation in Okotoks.

Solar radiation is more intermittent than outdoor temperature, which makes accurate hourly predictions harder to achieve. This point is illustrated by these examples:

- September 26th: the forecasts failed to predict significant solar irradiance fluctuations.
- September 30th: solar irradiance was overestimated significantly by the earlier forecasts (48-hr ahead). These values were corrected to some extent by the 6-hr forecasts, but there was still some overestimation.

On the other hand, on sunny days (e.g., September 27th to September 29th), solar radiation forecasts are quite accurate although an overestimation is clearly noticeable. Since cloud coverage and albedo are obtained from Environment Canada, CanMETEO perform calculations to evaluate the solar radiation by using the Perez sky modelling algorithms (Perez et al., 1990), which might cause the observed difference during sunny days. Such overestimation has been discussed in the DLSC Annual Reports (Leidos Canada, 2014) where measured data is compared on an annual basis (i.e., including sunny and cloudy days) with CWEC files, based on the same calculation approach. The authors of the report evaluated the annual deviation for the first seven years of operation and obtained CWEC values 10% higher than measured ones on average. It is clear that the overestimation of forecasted solar radiation might also be caused by other effects, including improper calibration or even physical aspects that have not been considered (e.g., air quality, accumulation of dust on the pyranometer, etc.).

To rectify solar radiation forecasts, a post-processing procedure can be applied by introducing a correction factor (CF) that automatically adjusts the predicted values, as follows:

$$CF[\%] = 100 \times \frac{SR_{\text{period}}^{\text{meas}}}{SR_{\text{period}}^{\text{fore,raw}}} \quad (5)$$

$SR_{\text{period}}^{\text{meas}}$ and $SR_{\text{period}}^{\text{fore,raw}}$ are the measured and raw forecast solar irradiance for a given period. The post-processing simply consists of multiplying the raw forecasts by the CF calculated over a carefully selected evaluation period.

As mentioned in Section 3.1, solar radiation forecasts should be assessed by comparing the total energy received over a certain period. Since the solar radiation overestimation is more noticeable (and more important) on sunny days, the post-processing correction should be applied based on these conditions (for example, two sunny days). Seasonal variation of correction factors might also be considered. In this paper, July 3-4 was used to calculate the correction factor. Predictions 6-hr ahead (the most accurate forecast available) were used. Results for corrected solar radiation forecasts are shown in Figure 9; a scatter plot is shown in Figure 10. In comparison with Figure 8, there is a clear improvement for sunny days, while larger deviations are still noticeable on cloudy days.

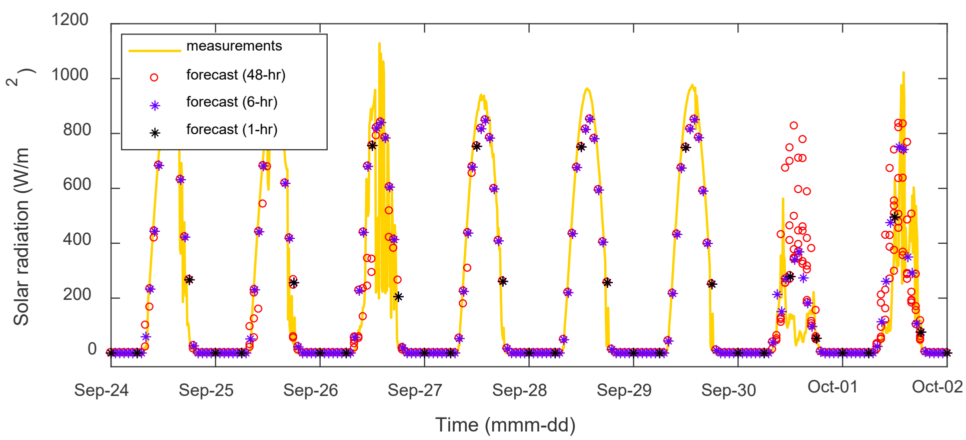


**Figure 9.** Post-processed forecasts: due South, 45°-tilted solar irradiance in Okotoks.

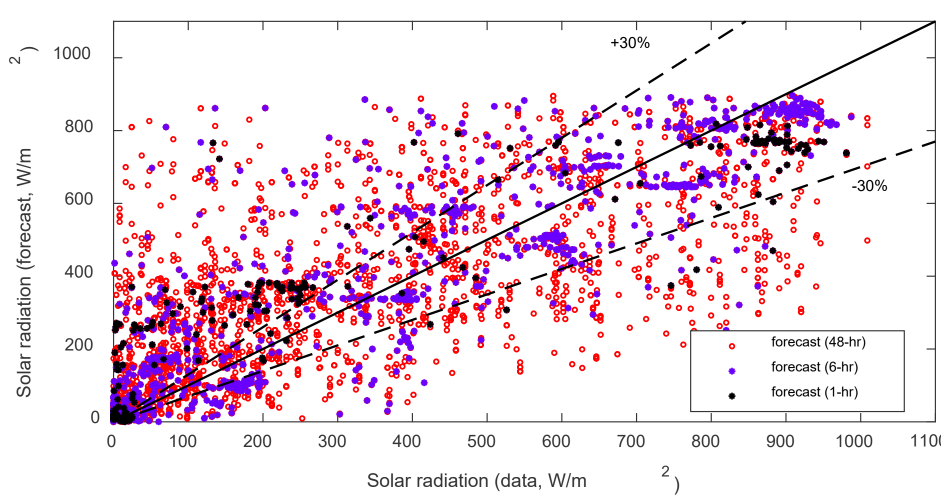


**Figure 10.** Comparison between post-processed forecasts and data for 45°-tilted solar radiation in Okotoks.

Further insight can be gained with a histogram of the difference between the post-processed predicted and measured radiation (Figure 11). The mean value of the error is 17 W/m$^2$, and the standard deviation is 167 W/m$^2$. About 78%

of the error values are within ±167 W/m² (better than a normal distribution with the same mean and standard deviation). Although in terms of percentage the difference seems larger on cloudy days (when the irradiance values are lower), the solar radiation is predicted reasonably well when it matters the most (i.e. on sunny days).

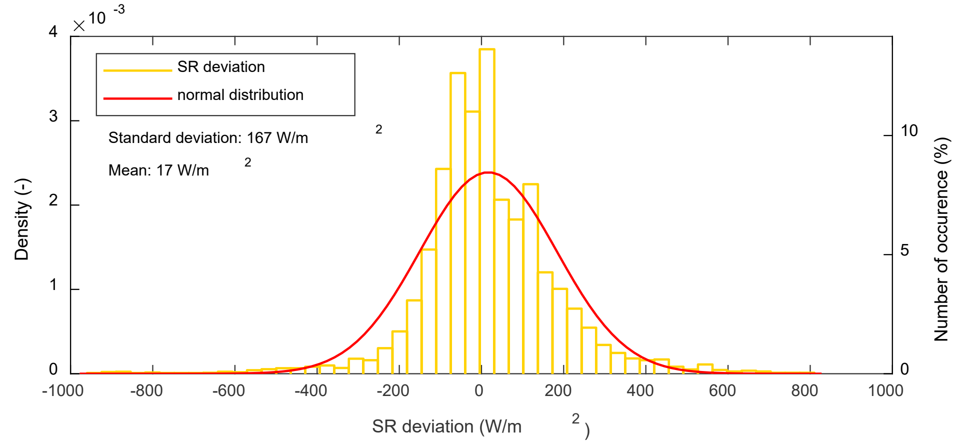


**Figure 11.** Histogram of solar radiation errors (post-processing predicted – measured).

As for the post-processing procedure, the accuracy of solar radiation was estimated by evaluating the total energy received over a certain period. Horizons of 6, 24 and 48 hours were selected and, normalized root-mean-square deviation ($NRMSD_j$) and overall deviation have been calculated. They are defined as follows:

$$NRMSD_j[\%] = \frac{100}{\overline{SR_j}^{\text{data}}} \sqrt{\frac{1}{N_{SR}} \sum_{i=1}^{N_{SR}} \left( SR_{i,j}^{\text{fore}} - SR_{i,j}^{\text{meas}} \right)^2} \tag{6}$$

$$\varepsilon_{\text{ov},j}[\%] = 100 \times \frac{\sum_{i=1}^{N_{SR}} \left( SR_{i,j}^{\text{fore}} - SR_{i,j}^{\text{meas}} \right)}{\sum_{i=1}^{N_{SR}} SR_{i,j}^{\text{meas}}} \tag{7}$$

where $SR_{i,j}^{\text{meas}}$ and $SR_{i,j}^{\text{fore}}$ are the measured and predicted solar radiation received over the horizon $j$ (e.g., 6-hr, 24-hr or 48-hr) when starting at time $t_i$. The variable $\overline{SR_j}^{\text{meas}}$ represents the average value of the solar radiation received over the horizon $j$ for the entire period (July 1st to December 31st). $N_{SR}$ refers to the number of times when measurements and forecasts were compared. Table 2 shows the results for raw and corrected forecasts for both sites. Low irradiance values were removed to avoid the effects of significant relative errors at low irradiance.

**Table 2:** Accuracy of 45°-tilted solar radiation forecasts (July 1st to December 31st).

| Indicator* | Horizon | Okotoks (AB) | | Varennes (QC) | |
|---|---|---|---|---|---|
| | | Raw | Corrected | Raw | Corrected |
| Normalized RMSD | 6-hr | 58.3% | 31.8% | 40.2% | 35.4% |
| | 24-hr | 46.9% | 24.6% | 34.0% | 28.8% |
| | 48-hr | 43.7% | 20.7% | 30.2% | 24.9% |
| Overall deviation | 6-hr | 36.9% | 4.7% | 24.0% | 14.8% |
| | 24-hr | 34.0% | 2.3% | 18.8% | 10.0% |
| | 48-hr | 32.7% | 1.2% | 16.1% | 7.5% |

* Values lower than 150 Wh/m² estimated over the next horizon have been neglected

Table 2 shows that the post-processing with CF improves the accuracy for all horizons and both locations. For Okotoks, the correction factor was estimated to 76.3%; for Varennes, it was 92.6%. As previously mentioned, this difference can be explained by several reasons (e.g., improper pyranometer calibration, effects of air quality, or differences in weather variability in the two locations). Even if the normalized RMSD seems quite high, the overall deviation is always positive (i.e., overestimation); after the post-processing procedure, the error is relatively low for predictions. Overall, the CF helps reduce deviations, especially in Okotoks. Finally, it is worth mentioning that higher NRMSD values were obtained with the 6-hr period; smaller cumulative values yield higher relative errors.

Histograms of the difference between the predictions and measurements for the solar energy received over a certain period of time is also given in Figure 12 for periods of 6, 24 and 48 hours. This information is of great interest, as it provides an estimation of the uncertainty associated to the solar energy received for the next few hours.

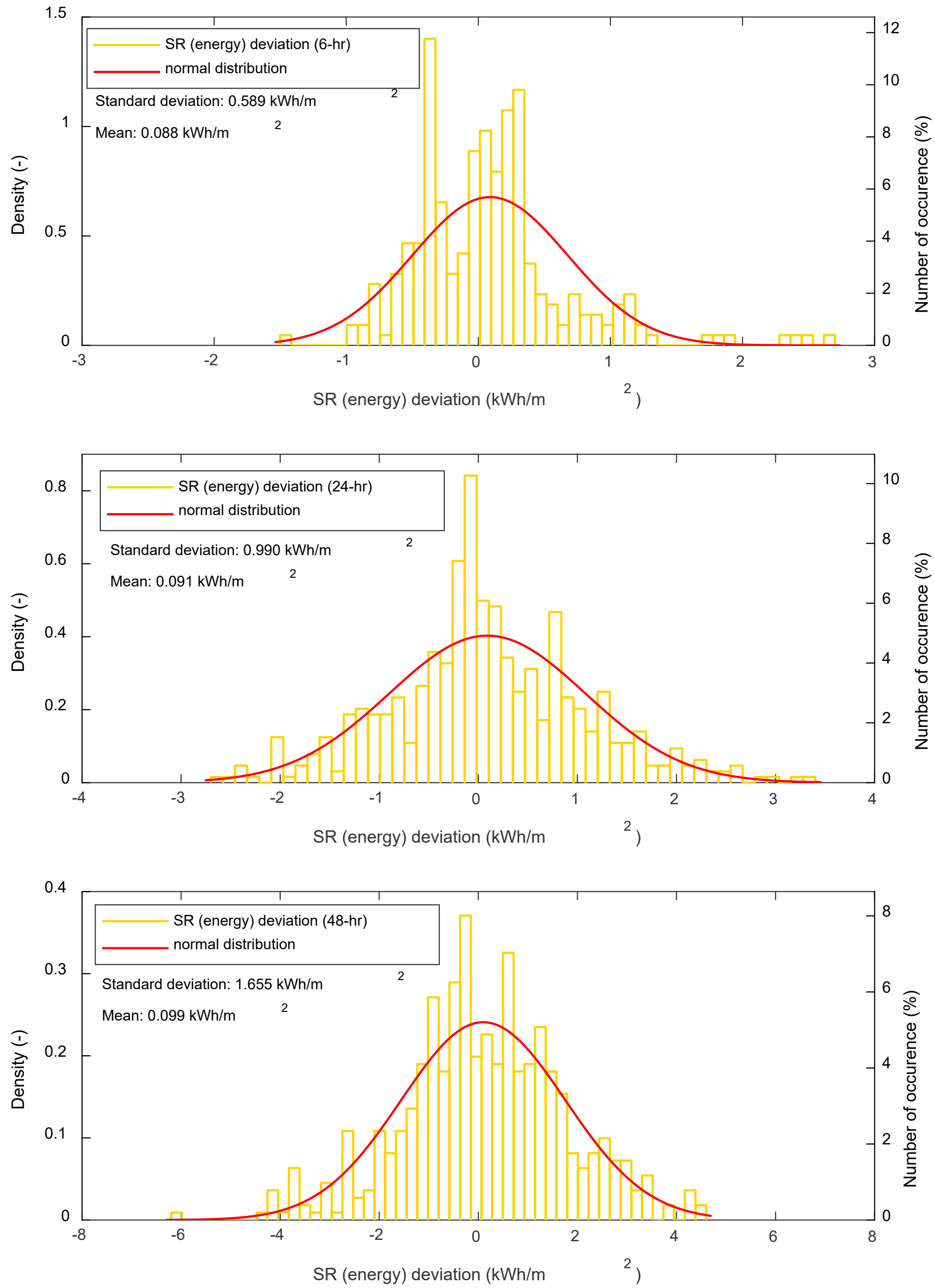

**Figure 12.** Histogram of the error (post-processed forecast – measured) of solar energy received for the next 6-hr (top), 24-hr (middle) and 48-hr (bottom).

In summary, in comparison with the accuracy and reliability of temperature forecasts, solar radiation is rather challenging, but it can still be reasonably estimated within a certain confidence interval. The application of this information for decision-making in building operation (i.e., weather forecasts and accuracy) is discussed below.

## 4. ROLE OF FORECASTS IN BUILDING OPERATION

The application of model-based predictive control for the operation of HVAC systems in buildings requires a model of the building and its systems, along with a reasonable prediction input data. The input information usually involves two distinct data sets: (a) information about weather, such as outdoor temperature, weather and solar radiation; (b) direct or indirect information about internal heat gains (e.g., occupancy, plug load profiles, etc.). The relative influence of weather is particularly important in homes, small and medium commercial buildings, and large buildings with a large ratio of outdoor surfaces to volume (i.e., high rise office buildings). The impact of weather is also clearly noticeable in perimeter zones, e.g. in offices with large windows.

Each of the steps of predictive control –modeling (Maasoumy et al., 2014), weather forecast (Petersen and Bundgaard, 2014), occupancy profiles and internal loads (Yan et al., 2015)– introduces uncertainty in the expected response of the building. One must remember that, while an accurate prediction is highly desirable, these pieces of information are meant to assist in the numerous decisions made by the building automation system (BAS). Therefore, an "imperfect" forecast can still yield useful results, as long as the level of uncertainty involved is taken into account in the control strategies. For instance, the predictions obtained for hourly values of solar radiation are within ±167 W/m$^2$ of the actual value. This information can be used in the planning of control strategies. For example, if the total radiation predicted for the next day is 5 kWh/m$^2$, a conservative approach could consist of using a value of 4 kWh/m$^2$ in the calculation of the output of building-integrated photovoltaic panels, or in the estimation of solar gains. The effect of solar irradiance on buildings depends on many factors (e.g., window-to-wall ratio). At the time of writing, the development team was working on improvements of this tool, and on its application in predictive control studies. Methods based on total sky imagery, satellite cloud motion or stochastic analysis could be used to improve short-term forecasts (Pelland et al., 2013), and better assess the impact of forecasts uncertainties.

## 5. CONCLUSION

This paper has presented a preliminary assessment of CanMETEO, a free-of-charge weather forecast tool focusing on the incorporation of predictive control in buildings. A brief discussion of the features of this tool –which currently produces data for the Canadian territory–, has been presented. The solar radiation calculations are obtained from calculations using the raw output of numerical weather predictions. An assessment of the accuracy of temperature and solar irradiance forecasts was made for two sites: Okotoks (Alberta) and Varennes (Québec).

Future work on this tool could potentially include the introduction of a user-defined correction factor for solar radiation. This correction factor could be changed seasonally. If a given site has readily available measurements, an upgrade in the tool could use this data to correct its predictions. Ensemble weather forecasts (i.e., the results of models with slightly different initial conditions) may provide an indication of the

Other potential upgrades of this tool include the development of predictive control strategies based on expected weather conditions. These strategies include the control of the thermal energy storage device of a district heating network in the town of Okotoks and the development of optimal temperature setpoints for the building located at Varennes. Giving the user the possibility to include installed PV capacity, fenestration size and other parameters would allow the tool to provide estimates of PV power output and solar thermal gains in building.

## ACKNOWLEDGMENTS

The authors would like to thank Mojtaba Samimi for his valuable inputs on the development of the tool. The comments of Lewis Poulin, Franco Petrucci and the team from Environment Canada is gratefully appreciated. We would like to thank the Office of Research and Development of Natural Resources Canada for the financial support of this study through the projects L-BE2-09 and EU-BE-11. The valuable comments of the internal and external reviewers of this document are gratefully acknowledged.

## REFERENCES

Aswani, A., Master, N., Taneja, J., Culler, D., and Tomlin, C. (2012). "Reducing transient and steady state electricity consumption in HVAC using learning-based model predictive control." *Proceedings of the IEEE*, 100(1), 240–253.

Bauer, P., Thorpe, A., and Brunet, G. (2015). "The quiet revolution of numerical weather prediction." *Nature*, 525, 47–55.

Candanedo, J., Paradis, E., and Stylianou, M. (2013). "Building simulation weather forecast files for predictive control strategies." *SimAUD 2013*, San Diego, CA.

*CanMETEO*. (2017). English / French, Natural Resources Canada.

Corbin, C. D., Henze, G. P., and May-Ostendorp, P. (2013). "A model predictive control optimization environment for real-time commercial building application." *J. of Building Perf. Simulation*, 6(3), 159–174.

Drgoňa, J., Picard, D., Kvasnica, M., and Helsen, L. (2018). "Approximate model predictive building control via machine learning." *Applied Energy*, 218, 199–216.

Duffie, J. A., and Beckman, W. A. (2006). *Solar Engineering of Thermal Processes*. John Wiley & Sons, Hoboken, New Jersey.

Hu, J., and Karava, P. (2014). "Model predictive control strategies for buildings with mixed-mode cooling." *Building and Environment*, 71, 233–244.

Killian, M., and Kozek, M. (2016). "Ten questions concerning model predictive control for energy efficient buildings." *Building and Environment*, 105, 403–412.

Leidos Canada. (2014). *Drake Landing Solar Community: Annual Performance Monitoring Report for 2013-14*. Annual Performance Monitoring Report.

Maasoumy, M., Razmara, M., Shahbakhti, M., and Vincentelli, A. S. (2014). "Handling model uncertainty in model predictive control for energy efficient buildings." *Energy and Buildings*, 77, 377–392.

Oldewurtel, F., Parisio, A., Jones, C. N., Gyalistras, D., Gwerder, M., Stauch, V., Lehmann, B., and Morari, M. (2012). "Use of model predictive control and weather forecasts for energy efficient building climate control." *Energy and Buildings*, 45, 15–27.

Pelland, S., Remund, J., Kleissl, J., Oozeki, T., and De Brabandere, Karel. (2013). "Photovoltaic and solar forecasting: state of the art." *Report IEA-PVPS Task 14*.

Perez, R., Ineichen, P., Seals, R., Michalsky, J., and Stewart, R. (1990). "Modeling daylight availability and irradiance components from direct and global irradiance." *Solar Energy*, 44(5), 271–289.

Petersen, S., and Bundgaard, K. W. (2014). "The effect of weather forecast uncertainty on a predictive control concept for building systems operation." *Applied Energy*, 116, 311–321.

Samimi, M. (2015). *Turbidity factor calculation*. Personal communication.

Sibbitt, B., McClenahan, D., Djebbar, R., Thornton, J., Wong, B., Carriere, J., and Kokko, J. (2012). "The Performance of a High Solar Fraction Seasonal Storage District Heating System – Five Years of Operation." *Energy Procedia*, 1st International Conference on Solar Heating and Coolingfor Buildings and Industry (SHC 2012), 30, 856–865.

Stauch, V., Hug, C., Schubiger, F., and Steiner, P. (2010). "Weather forecasts, observations and algorithms for building simulation and predictive control." *Zürich: MeteoSwiss*.

Yan, D., O'Brien, W., Hong, T., Feng, X., Gunay, H. B., Tahmasebi, F., and Mahdavi, A. (2015). "Occupant behavior modeling for building performance simulation: Current state and future challenges." *Energy and Buildings*, 107, 264–278.